Eur. Phys. J. Spec. Top. (2024) 233:1695–1708
https://doi.org/10.1140/epjs/s11734-024-01243-x

THE EUROPEAN PHYSICAL JOURNAL SPECIAL TOPICS

Regular Article

Influence of ultrasound on the dynamics of an air bubble near a solid surface

Michael O. Kuchinskiy[1,2,a], Tatyana P. Lyubimova[1,2,b], Konstantin A. Rybkin[2,c], Vasiliy A. Galishevskiy[2,d], and Anastasiia D. Sadovnikova[2,e]

[1] Institute of Continuous Media Mechanics UB RAS, 1, Koroleva Street, Perm 614013, Russia
[2] Perm State University, 15 Bukireva str., Perm 614068, Russia

Received 17 January 2024 / Accepted 1 July 2024 / Published online 15 July 2024
© The Author(s), under exclusive licence to EDP Sciences, Springer-Verlag GmbH Germany, part of Springer Nature 2024

Abstract In many technological processes, wettability plays an important role. There are various methods to control the wettability. The use of ultrasound can be used as one of the methods that allows to change the wetting angle and accordingly affect the wettability of the surface. In this paper, we study the effect of ultrasound on the solid surface–liquid–air bubble system. The solid plates of various degrees of wettability (quartz, acrylic, and Teflon plates) are used as the solid surfaces in experiments. The air bubble has a characteristic size of the order of ~ 1 mm. It is found that in the case of quartz plate, when exposed to ultrasound, the bubble is not fixed on the plate, a thin liquid layer remains between them. Since the acoustic pressure is non-uniform along the plate surface due to the reflection of ultrasonic waves from the container walls and the free surface of the water, being near the surface of the quartz glass plate, the bubble is displaced into an area of lower acoustic pressure and oscillates there. In the case of acrylic and Teflon plates, the bubble is fixed on the solid surface, and its surface oscillates with a frequency equal to the frequency of shape mode 2 eigen oscillations. The dependencies of the contact diameter, contact angle, and height of the bubble on the time of ultrasonic exposure are obtained for solid surfaces of different degrees of wettability. The change in wettability in ultrasound field is recorded for the acrylic and Teflon surfaces such that after 10 s of ultrasonic exposure and switching off the ultrasound, the reduction of the contact angle is detected.

1 Introduction

Wettability in the scientific and technological fields is an important characteristic of the surface of the material [1]; it is determined by a force balance between the adhesive and cohesive forces [2, 3]. The numerical characteristic of wettability is the contact angle (wettability angle). Various methods are used to determine the contact angle: oscillating droplet, sessile drop, captive bubble [4, 5]. In measurements using the sessile drop method, a drop of water located on the surface in the air is considered, so a three-phase system is formed in which it is possible to fix the visible angle between the boundaries of the solid–liquid and liquid–gas phase. Other studies use the captive bubble method. In this case, a gas bubble in the liquid phase on a solid surface is considered: this method allows to track changes in its shape, micro-flows near the surface of the bubble, motion of the center of mass, and dynamics near a solid surface.

In many technological processes, such as soldering, inkjet printing, coating, and separation, it is necessary to control the wettability of the surfaces involved. A review [6] demonstrated that, with increasing temperature, the contact angle between a liquid and a solid decreases, whereas the rate of change in angle also increases. There are

Michael O. Kuchinskiy, Tatyana P. Lyubimova, Konstantin A. Rybkin, Vasiliy A. Galishevskiy and Anastasiia D. Sadovnikova have contributed equally to this work.

[a] e-mail: kat6chinskiy@gmail.com
[b] e-mail: lyubimovat@mail.ru (corresponding author)
[c] e-mail: k.rybkin@gmail.com
[d] e-mail: ifonlyheknow@yandex.ru
[e] e-mail: anastasiiia3006@mail.ru

also alternative ways to influence wettability: in the work of Liu et al. [7], the hydrophilicity of coal was increased by using surfactants. Its addition increases the interaction of water with coal and the diffusion coefficient of water molecules, which leads to the transformation of the surface of coal from hydrophobic to hydrophilic. However, traditional methods that allow for changing the contact angle have a number of disadvantages. In the first case, a large amount of energy is required for heating. In the second case, the liquid is a mixture of two components (surfactants and water), which entails a number of environmental problems.

The solution to these problems may be the use of external mechanical means, including ultrasonic exposure [8, 9]. Ultrasonic waves can have both positive and negative impacts on technological processes, as they affect hydrophilic and hydrophobic surfaces in various ways. In the work of Fillipov et al. [10], the influence of ultrasound on the flotation process was investigated. It was discovered that the process of bubble attachment to ore particles occurred selectively, as the wettability of NaCl and KCl particles differed and changed during ultrasonic treatment due to the desorption of surfactants.

When using ultrasound to modify contact angles, there are no associated difficulties with high energy consumption or environmental harm. At the same time, using intense exposure to ultrasound allows for quick changes in the contact angle. This requires comprehensive theoretical and experimental investigation. When measuring the contact angle using the sessile drop method, it is often considered that the effect of a solid surface oscillating with ultrasonic or lower frequencies on which the drop is located can influence the measurement [11–14]. For example, in the work of Sarasua et al. [15], a thermodynamic model was developed to describe the hysteresis of contact angle in a three-phase system of solid, liquid, and air, specifically the decrease of contact angle under the influence of ultrasound. In a study [16], it is observed that wettability can be controlled by varying the speed, frequency, and amplitude of ultrasonic vibrations.

The inverted task, in which the measurement of the contact angle under the action of ultrasound is performed by the captive bubble method, is considered less often, but is also relevant. A number of phenomena occur during ultrasonic exposure, so there is a wide range of research dedicated to the behavior of bubbles in liquid under the influence of vibration.

The Bjerknes force acts on a bubble from the acoustic field, which can contribute to its movement and interaction with other bubbles. In the presence of bubbles of different sizes in a liquid, the primary Bjerknes force in a standing acoustic wave separates them by size in such a way that smaller bubbles accumulate at pressure antinodes and larger bubbles at pressure nodes [17]. In the case of two bubbles, a secondary Bjerknes force arises due to the appearance of a secondary acoustic field emitted by an oscillating bubble [18–20]. Depending on the phase of the bubble oscillation, the secondary force can lead either to coalescence (fusion) or repulsion. Additionally, external ultrasonic exposure can lead to shape oscillations of the bubbles [21–23], and can lead to the formation of nanobubbles in the liquid through cavitation. When a solid surface is present in a liquid, these phenomena can affect the wetting properties of the material [24].

In our paper, the interaction of an air bubble with hard surfaces of varying degrees of hydrophobicity (quartz, acrylic and Teflon) under the influence of an ultrasonic field is investigated. We conducted experiments that are partially presented in the present paper and determined the general features of the behavior of gas bubbles under ultrasonic exposure at different time scales. For the first time, the dependences of the instantaneous characteristics of a bubble in contact with a solid surface (dynamic contact angle, height and diameter of the contact) on time on a short time scale were obtained using the captive bubble method. A decrease in the static contact angle due to prolonged ultrasonic exposure was also detected.

2 Description of the experimental setup and data processing methodology

The experiments used a cuvette shaped like a parallelepiped with dimensions $103 \times 103 \times 195\,\text{mm}^3$ (Fig. 1). The cuvette was made of 3 mm thick acrylic glass, a 28 kHz ultrasonic flat transducer with a power of $P = 32\,\text{W}$ was installed at the base. In the upper part of the cuvette, at a depth of 20 mm from the surface of the liquid, a plate made of the material under study (quartz, acrylic, Teflon) was fixed strictly horizontally. Basler acA1920-155um SSD camera was used to register and measure the contact angle (sensor size $11.3 \times 7.1\,\text{mm}^2$, resolution (H × V pixels) 1920 $px \times 1200\ px$, pixel size $(H \times V)$ 5.86 $\mu m \times 5.86\ \mu m$, frame rate 164 fps), together with a collimated contour light source Telecentric HP illuminator (peak wavelength blue, 460 nm; power consumption $P < 2.5\,\text{W}$), equipped with telecentric macro lenses.

This optical system made it possible to measure the size of bubbles regardless of the distance between them and the camera matrix. The minimum size of the fixed bubble for this optical scheme was $\sim 32\ \mu\text{m}$, while the depth of field was 2 cm.

The Basler A504kc high-speed camera was used to measure the frequency of bubble oscillations and the LED backlight source with a power of $P = 30\,\text{W}$. The shooting frequency in this case was 5000 fps resolution 1280 px × 102 px. Due to the fact that the ultrasonic frequency is 28 kHz, and the frame rate is reported to be 5000 fps, the time resolved dynamics cannot be fully recorded.

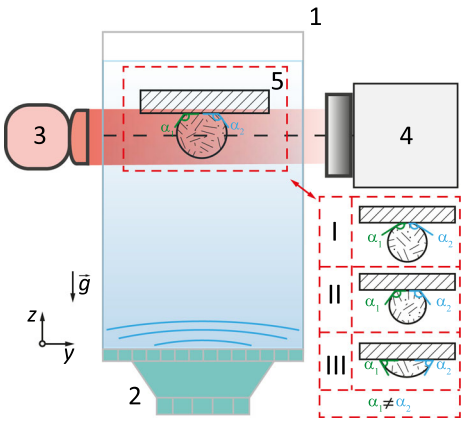


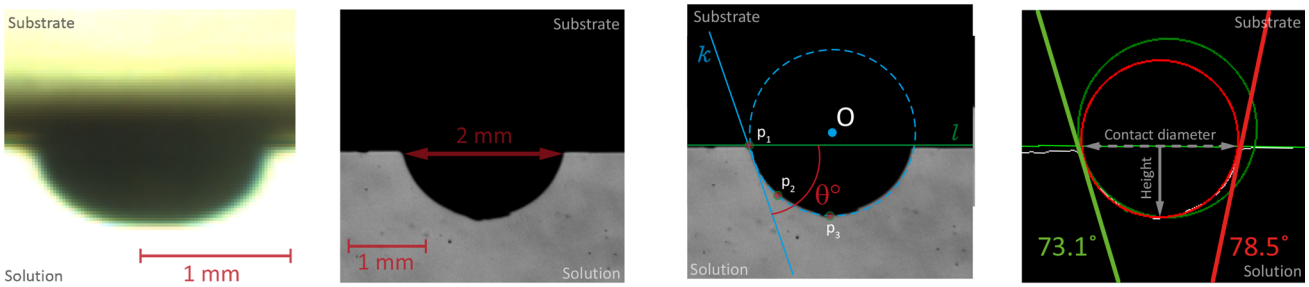
Fig. 1 Experimental setup: (1) the acrylic glass cuvette $103 \times 103 \times 195\,\text{mm}^3$; (2) the ultrasonic flat transducer $f = 28\,\text{kHz}$ with a power of $P = 32\,\text{W}$; (3) light source; (4) camera; (5) the test surface (quartz, acrylic, Teflon). The scheme on the right side of the figure shows the difference in contact angle depending on hydrophilicity (I—quartz, II—acryl, III—Teflon)

For the experiments, distilled water at room temperature was used, which was kept for at least a day in an open vessel in the immediate vicinity of the experimental site and solid plates of three types: amorphous quartz, acryl, and Teflon. Plates with varying degrees of hydrophilicity were placed in the experimental setup. This made it possible to trace the dynamics of the bubble under the influence of ultrasound, as well as to identify changes associated with changes in the degree of wettability of the surface, varying it from a hydrophilic surface (quartz) to an intermediate one (acryl) and ending with a relatively hydrophobic surface made of Teflon.

To create a bubble, a calibrated glass capillary was used, emitting single air bubbles using a piston pump. The size of the bubble varied within $1 \div 2\,\text{mm}$. Since the solid surface can change under the influence of ultrasound [25], the studied plates were replaced with identical ones after each experiment. Each series included ten similar experiments to establish a trend.

The photos obtained during the experiment (Fig. 2a, b) were processed using a Python algorithm developed on the basis of the tangential method of measuring the contact angle [26, 27]. At the first stage, the image was binarized so that only the contour of the bubble on the surface of the plate remained in the image, then the black color was assigned the value 0, and the white one – 1. As a result of these actions, a two-dimensional array of 0 and 1 was obtained, the elements of which were used in subsequent calculations. Next, in the picture (Fig. 2c), the plate line (l) and the maximum deviation from it corresponding to the upper point of the bubble (p_3) were determined, after which the extreme (p_1) and intermediate (p_2) points on the bubble boundary were searched. Next, the equations of the tangent circle at the extreme point of the bubble were written at three points. Then, using the equation of the straight line running along the plate and the equation of the tangent (k), the contact angle (Θ, °) was calculated. That is, the contact angle is the angle between the tangent to the circle and the line drawn along the plate.

As a result of each experiment, images were obtained, an example of which is shown in Fig. 2a, b. In Fig. 2c, the software processing is presented, the final result of the program is Fig. 2d.



(a) (b) (c) (d)

Fig. 2 An example of the resulting images and the result of their processing for an acrylic surface: **a** is the image obtained during the experiment using the Basler A504kc camera, **b** is the image obtained during the experiment using the Basler acA 1920-155 um camera, **c** Using a tangential processing method to measure the contact angle, **d** The result of software image processing

3 The results

3.1 Experiments with quartz glass surface

In experiments, a capillary was used allowing the creation of bubbles with a diameter of $1 \div 2$ mm. This size is significantly larger than the resonant size, which can be calculated using the formula [28, 29]:

$$R_r = \sqrt{\frac{3\gamma p_s}{\rho_f (2\pi f)^2}}, \tag{1}$$

where γ is the ratio of specific heats, p_s is the ambient static pressure, ρ_f is the density of the liquid, and f is the frequency of oscillations. The resonance size of the bubble calculated from Eq. (1) for air bubble in water at frequency of 28 kHz is $R_r \approx 0.12$ mm. In this regard, inertial cavitation effects (bubble collapse) occurring with bubbles of resonant size cannot be observed in this work.

As shown by experiments conducted with distilled water and quartz glass plates (the wetting angle is $130° \div 145°$) (hydrophilic surface), after formation, the bubble is not fixed on the solid surface.

This behavior of the bubble is due to the hydrophilicity of the quartz glass surface; it can be said that quartz plates completely immersed in water are well wetted with water, and as a result, a thin liquid layer immediately forms on its surface which prevents the bubble from fixing on the plate (Fig. 4).

A liquid layer, or as it is also called a wetting film, is formed both on hydrophobic and hydrophilic surfaces, but in the case of hydrophilic surfaces it is highly stable, while for hydrophobic surfaces the wetting films are significantly less stable [30–32]. In accordance with the DLVO theory (was named after Boris Derjaguin and Lev Landau, Evert Verwey and Theodoor Overbeek investigations), the stability of the liquid film can be considered as a balance between van der Waals (VDW) force and double layer forces (DLF) [30, 33], where the forces of the double layer (DLF) lead to repulsion, which occurs due to surface charges at the interface and the van der Waals (VDW) forces of attraction.

Therefore, the air bubble rising from the capillary to the solid plate does not have sufficient energy to rupture a stable liquid layer and does not fix on it when it hits the quartz plate. The formation of such a film can be seen in Fig. 3, where the images of a gas bubble taken in reflected light are presented for the surfaces of acrylic and quartz. In the case of acrylic plate, the bubble edge is clearly observed and in the case of quartz, there is a black ring, indicating that there exists a liquid layer between the bubble and solid surface that prevents the bubble fixing.

Due to above, in the case of quartz plate, the ultrasonic exposure leads to oscillations of the bubble shape and position near the solid surface (Fig. 4). The rebound of the bubble from a solid surface was also observed in [34]

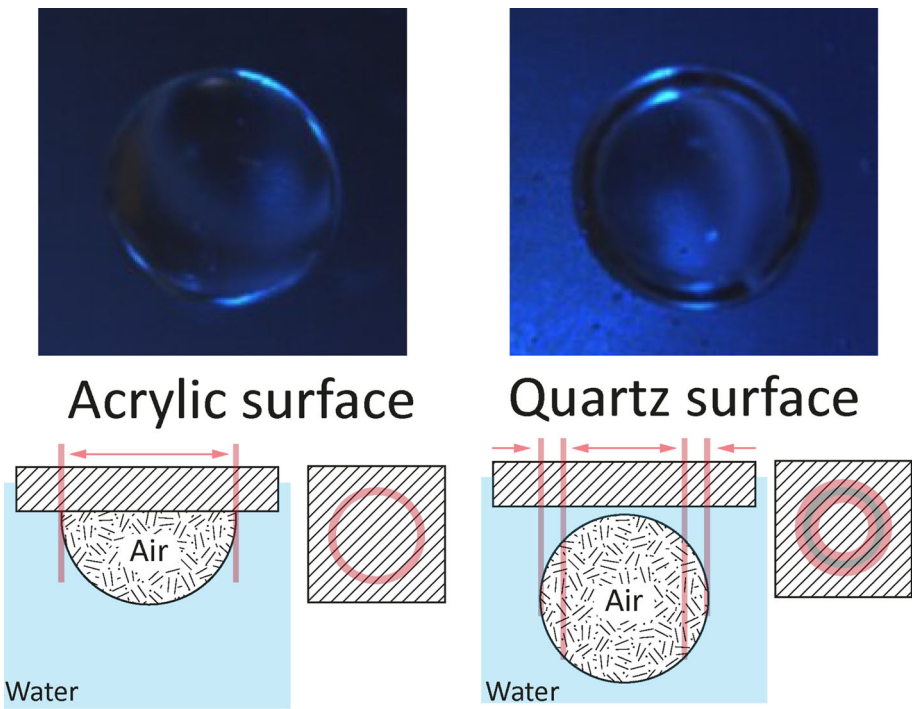


Fig. 3 Photos taken in reflected light for the air bubble in the Acrylic and quartz surface. The formation of a black ring on the surface of quartz is noticeable, indicating the presence of a liquid film

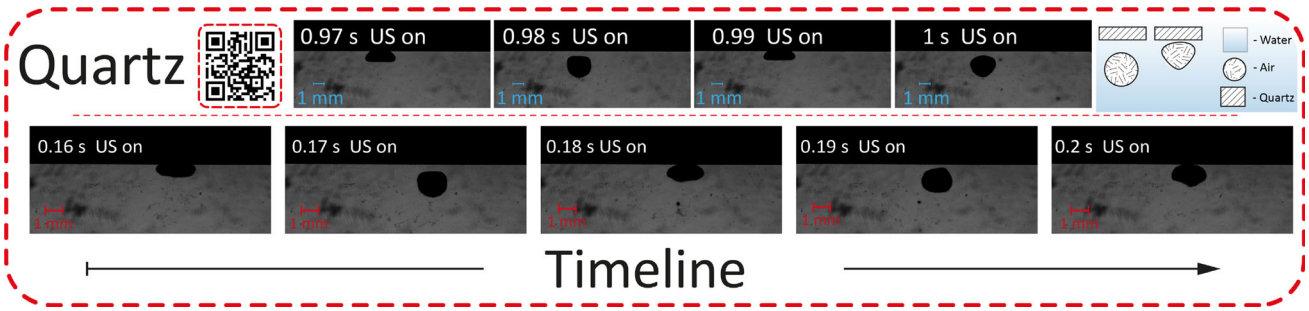
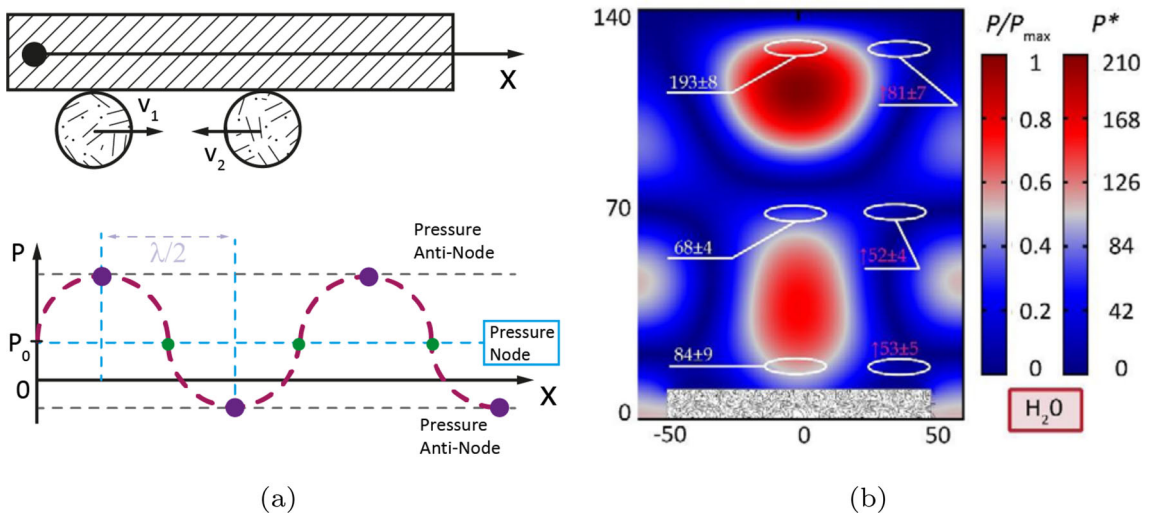


Fig. 4 Bubble oscillations near the quartz surface under the influence of ultrasound



(a) (b)

Fig. 5 Non-unity of the acoustic field inside the sonochemical reactor and near a solid surface, **a** schematic representation of acoustic wave near the rigid surface, **b** the numerical simulation results presented in the article [35] demonstrate the non-uniformity of the acoustic pressure distribution in a sonochemical reactor

in the absence of external fields.

Experiments with quartz plates have shown that under the action of anultrasound field, the bubble starts to slide along the plate into the area of the lower pressure—the node of the standing wave. This phenomenon shown in Fig. 5a was observed in [36], when, during the generation of a bubble using a capillary in the pressure anti-node (wave antinode), the bubble moved under the action of the acoustic field in the pressure node (wave node). In the case discussed in [36], the adhesion forces exceeded the acoustic ones, so the bubble did not detach from the capillary, and it assumed a stable position. In the present work, the bubble could move freely along the plate due to the hydrophilicity of the surface, so the bubble, having reached the area of low pressure, continued to oscillate near the plate. This is due to the fact that the field created in a liquid when exposed to ultrasound is spatially non-uniform [35, 37]; it is presented in Fig. 5b.

This inhomogeneity can be related both to the interference of waves reflecting from the rigid boundaries of the container, and to the presence of air bubbles in the liquid that occur in the path of wave propagation and change the acoustic impedance of the medium [22]. The manifestation of the inhomogeneity of the acoustic field is illustrated in Fig. 6. Regardless of the location of the bubbles relative to the quartz plate, when the ultrasound source was activated, and the bubble shifted to the area with low pressure. The interaction of two bubbles, which coalesced under the influence of Bjerknes forces, is shown in the case illustrated in Fig. 6.

3.2 Experiments with the acrylic surface

Acrylic was chosen as a material having an intermediate degree of wettability. According to the results of experiments without ultrasonic exposure, the contact angle on such a surface is in the range $92° \div 102°$. In the absence of ultrasonic action, the bubble is fixed on the surface of the acrylic; however when ultrasound is turned on, due to the predominance of Bjerknes forces over the adhesion forces, the fixation turns out to be unstable and the

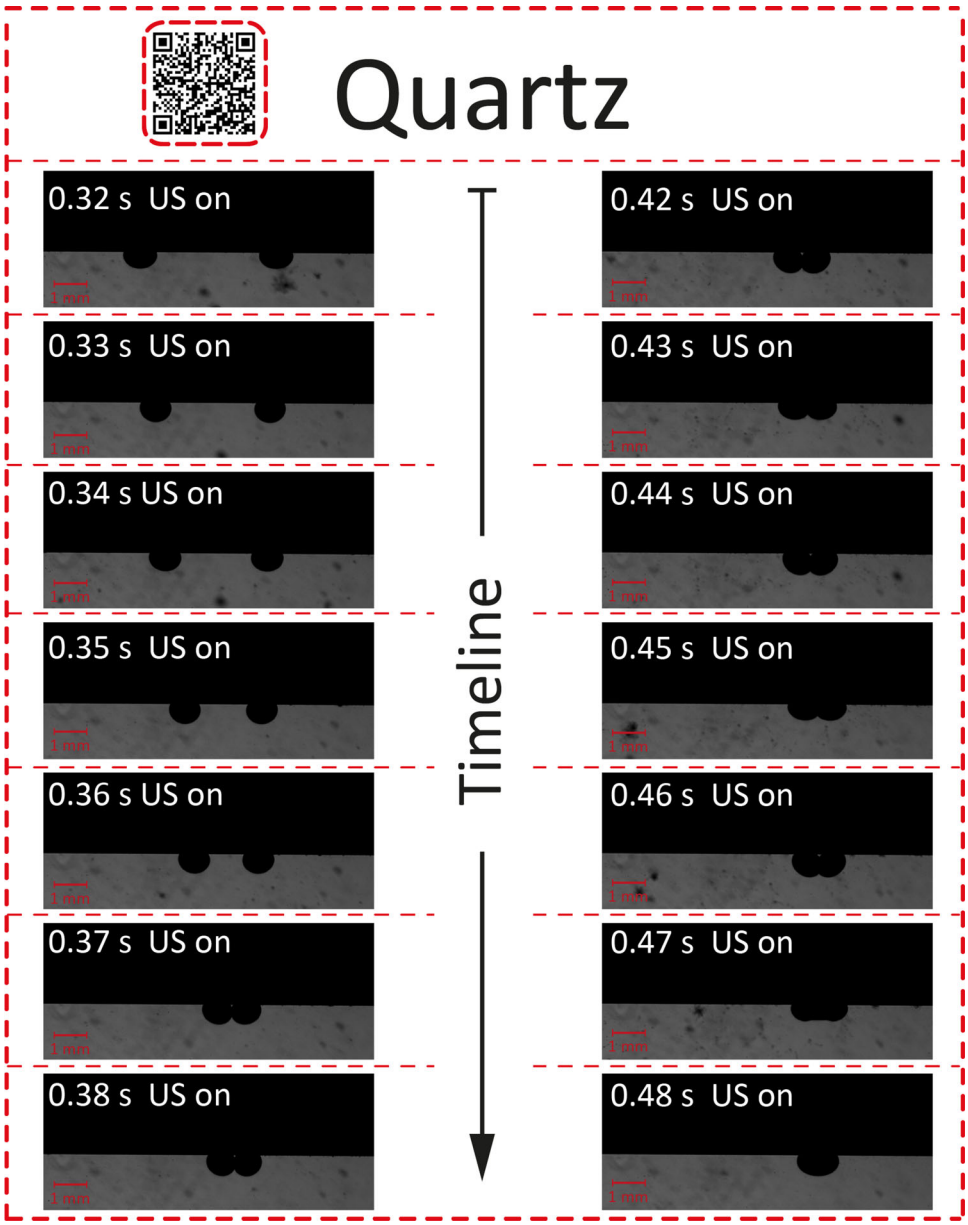


Fig. 6 The movement of two bubbles under the influence of ultrasound into an area of lower acoustic pressure and their subsequent coalescence on the quartz surface

bubble shifts to an area of low acoustic pressure where it is then steadily fixed. As a result, air bubbles were fixed on the acrylic surface, which was different from quartz. In experiments with quartz, bubble oscillated near the surface. However, the movement of the bubble along the plate surface to the lower pressure area related to the dominance of the Bjerknes forces over the adhesion forces holding the bubble in a fixed position is still possible and was observed in the experiments.

Translational oscillations of the bubble in the vertical direction near the plate surface, as occurred in experiments with quartz, are not observed due to the lower hydrophilicity.

Figure 7 shows images of bubbles on an acrylic surface, before and after exposure to ultrasound. The left-hand side of the figure shows the parameters of the bubble (contact angle, contact diameter, and height) before the ultrasound was applied, while the right-hand side shows 2 s after the ultrasound had been turned off and had lasted 10 s. These photos demonstrate the static angle that is formed when the bubble adheres to the acrylic surface. Fig. 8 shows the dependence of the static contact angle on the ultrasonic exposure time for 10/30/60 s on the acrylic surface. Figures 7 and 8 show that, as a result of a 10-s exposure to ultrasound, the contact angle of a bubble decreases by an average of 10%, regardless of the diameter of the bubble. With a longer exposure time, there is no clear trend in the dependence of contact angle on time. Subsequently, in addition to reducing the contact angle, its increase can also be observed.

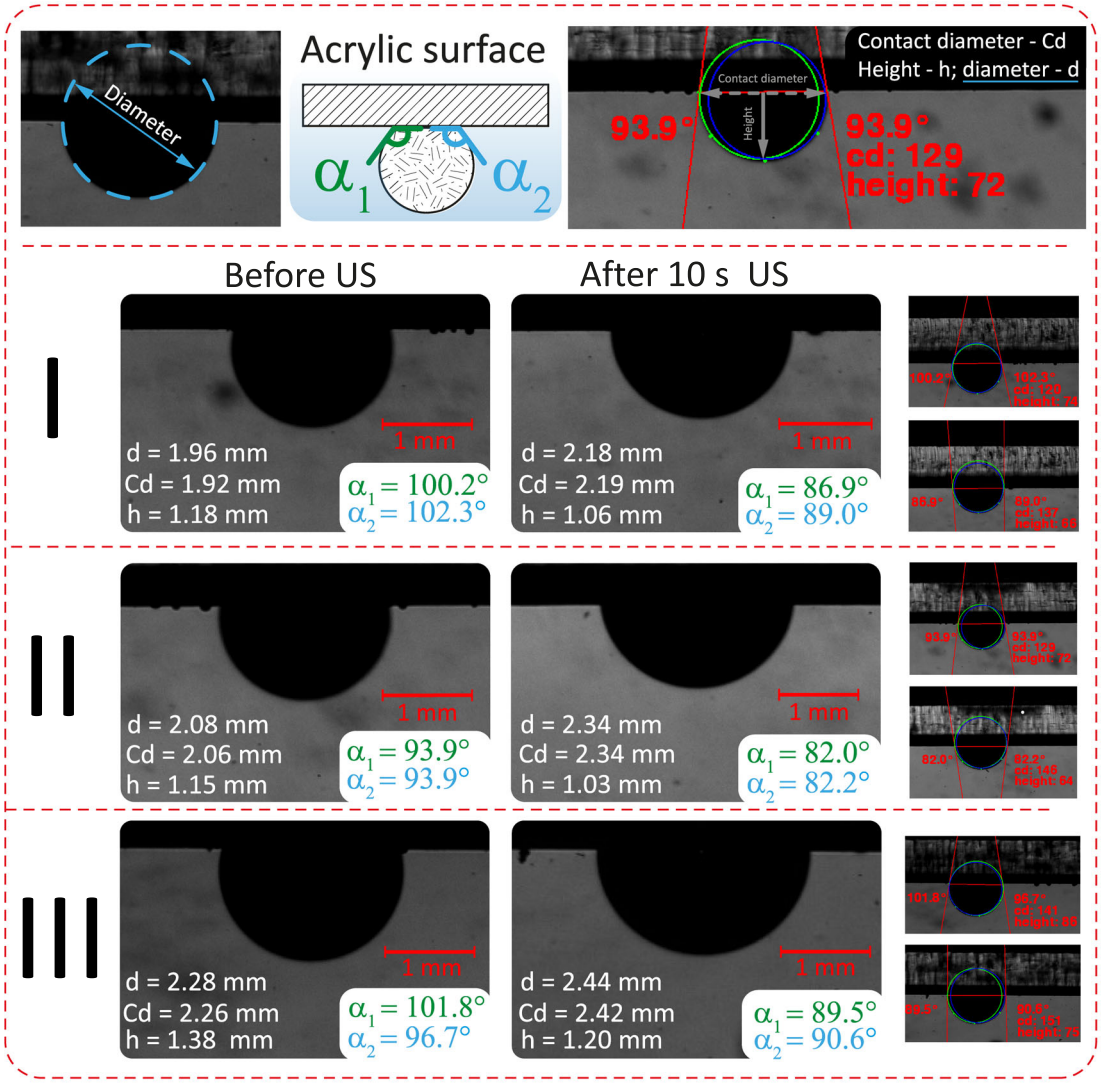


Fig. 7 A series of experiments showing a decrease in the contact angle as a result of 10-s ultrasonic exposure to an acrylic surface

The change in the contact angle in this case can be explained by the relation between the surface energy and the kinetic energy that the vibrations bring into the system which allows it to overcome the energy barrier (see, for example [15, 38, 39]) and reach the state of GEM (global minimum energy), which determines the contact angle. In [15, 40, 41], the hysteresis of the contact angle arising from vibrations is discussed. In these studies, it is investigated that the vibrations allow the drop to overcome the initial contact line caused by the surface roughness; as a result, the drop does not return to its original state when vibrations are turned off. That is, vibrations transfer the droplet from a metastable state with higher energy to a state with a lower one. The reason for the decrease in the contact angle in this work may be in that the bubble oscillations enable the contact line to pin to stronger defects in the solid structure and in the bubble mean shape deformation in the ultrasound field (bubble flattening in the direction of ultrasound wave propagation)

Some of the researchers [42, 43] who also detect the effect of US on the contact angle associate this with the other mechanisms: physical effects due to pressure waves and micro jets acting on a solid surface, and extreme temperatures and pressures creating highly reactive radicals interacting with and altering a solid surface.

One of the reasons for the change in the wetting angle may be a change in the distribution of electric charge near a solid surface as a result of the triboelectric effect [44, 45]: when a drop vibrates under the influence of ultrasound, a change in the double electric layer (EDL) occurs. The combined effect of oxygen radicals resulting from the effects of ultrasound and the redistribution of electric charge on a solid surface can cause noticeable changes in EDL, and hence the wetting angle. Thus, the aforementioned effects, which cause a change in the contact angle, also occur

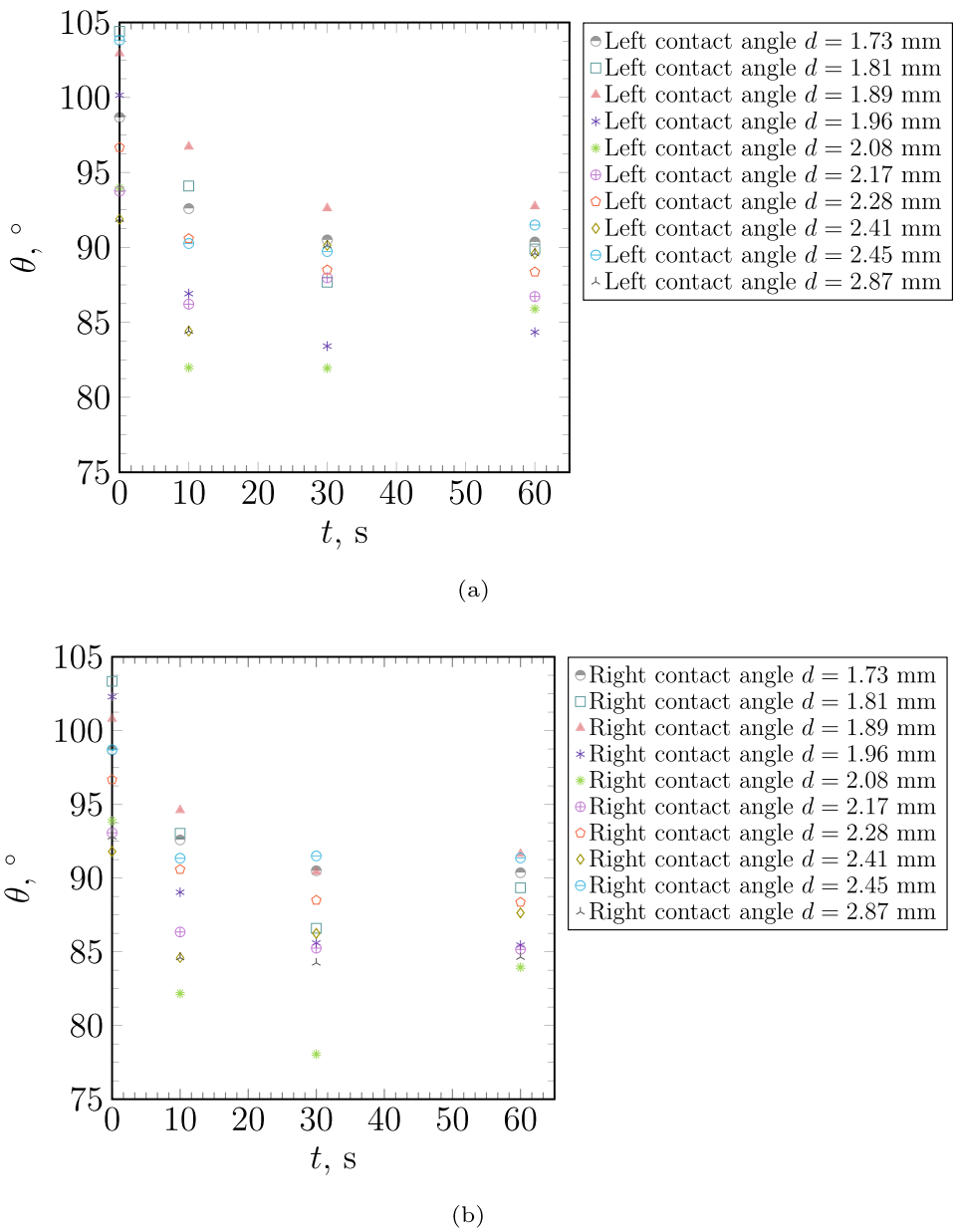


Fig. 8 Changing the static contact angle on the acrylic surface for different ultrasonic exposure times

in this work, despite the fact that the captive bubble method is used in the present problem (inverted by the one presented in [15, 40, 42–45]).

The decrease in the angle can be also related to the effect of rectified diffusion and coalescence with microbubbles, which is also observed with ultrasonic exposure. These phenomena are also responsible for the increase in the size of the bubble. Data before and after 10 s of ultrasound exposure are shown in Fig. 7.

The paper presents the results of measurements of the height and contact diameter of a bubble on an acrylic surface. Data were recorded for each series of experiments, and there was a general trend. Therefore, only the results for one bubble are presented here. Figures 9, 10 show the time evolution of the left and right contact angles, contact diameter, and bubble height (the distance between the extreme upper point of the bubble and the middle point of the contact diameter). In the experiments with quartz glass plates discussed in Sect. 3.1, it was impossible to measure these characteristics, since the bubble is not fixed on the quartz surface. As one can see, the oscillations of the wetting angles occur in phase with oscillations of the bubble height in this case, and the contact diameter oscillates in antiphase with the height (Fig. 9). This means that if the bubble is pressed against the surface, this leads to an increase in its diameter and a decrease in height, and at another stage the reverse process occurs, the diameter decreases and the height of the bubble increases.

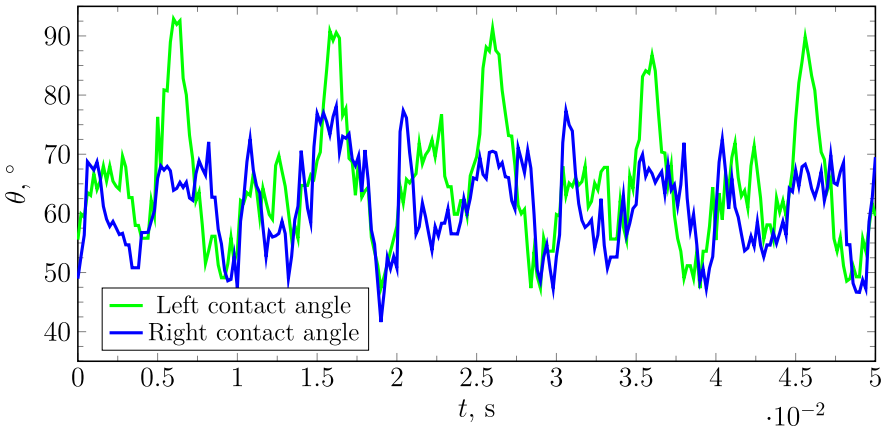


Fig. 9 Temporal dynamics of changes in the left and right contact angles on the acrylic surface under ultrasonic exposure

Oscillations of a bubble on a solid substrate under the action of spatially homogeneous pressure field pulsations are considered in [46]. It is shown that, as a result of interaction between a bubble and a substrate through a moving contact line, volume oscillations cause shape oscillations. In our case, the bubble size is $d \approx 2$ mm, and the distance from the antinode to node of the ultrasonic wave for the frequency 28 kHz is $\lambda/4 \approx 13$ mm. Therefore, the condition for the validity of the assumption of the acoustic pressure field spatial uniformity, $\lambda/4 >> d$, generally speaking, cannot be considered as fulfilled; therefore, the pressure field cannot be considered as spatially uniform. This is also confirmed by the experiment, where translational oscillations of the bubble parallel to the sound wave are observed. It is evident that such motion is not possible under spatial uniform pressure field. Thus, interaction between a bubble and a substrate leads to surface oscillations at a frequency equal to that of the mode 2 of the eigen shape oscillations, despite that in this work the pressure field cannot be considered spatially homogeneous.

The frequency of oscillations of the bubble height (Fig. 10) was compared with the frequency of eigen oscillations of the shape of an initially spherical bubble in an infinite vibrating liquid obtained neglecting the viscosity, gravity. and compressibility (see, for example, [23, 47]):

$$\omega^2 = \frac{k(k^2-1)(k+2)\alpha}{(\rho_l k + \rho_g(k+1))R^3}, \tag{2}$$

where $k = 2$ is the oscillation mode number, ρ_l is the density of the liquid, ρ_g is the density of air, α is the surface tension at the boundary of the water–air interface, and R is the average bubble radius; however, in the present experiment, the bubble is not incompressible. By substituting $R = 0.8 \cdot 10^{-3}$ m (diameter - $d = 1.6$ mm), $\rho_l = 1000$ (kg/m^3), $\rho_g = 1$ (kg/m^3), $\alpha = 0.073$ (N/m), we obtain for the angular frequency of eigen oscillations with $k = 2$ the value $\omega = 2\pi f = 416\pi$, i.e., $f = 208$ Hz. In experiments, the shape oscillations frequency was found to be 208 Hz, which matches with the theoretical value obtained from Eq. (2). Thus, it can be observed that the surface of the bubble oscillates at a frequency equal to the frequency of its shape mode 2 eigen oscillations.

On the experimental graph of the dependence of the height of the bubble on the time of ultrasonic exposure (Fig. 10), you can also see the alternation of large and small peaks. This phenomenon is associated with the presence of several harmonics of bubble oscillations [48], resulting from the interference of waves generated by the ultrasound source with the waves reflected from the walls of the cell, the air–water interface, etc.

3.3 Experiments with the surface of Teflon

The material representing the most hydrophobic surface used in the experiments was Teflon; according to the measurements, in the absence of ultrasound, the wetting angle on plates made of this material was $65° \div 75°$.

It should be noted that even with the highest degree of hydrophobicity of the plate (among the studied surfaces), the air bubble is displaced to the region of low acoustic pressure (similar to the situation on the glass surface—Fig. 6), i.e., into the node of the standing wave, with subsequent oscillations of the bubble surface. As in the experiments with acrylic, there was no detachment of the bubble from the rigid surface, so a series of experiments similar to acrylic was carried out.

Experiments have shown that as a result of continuous 10-s exposure to ultrasound, a change in the contact angle occurs—Fig. 11 (values are fixed after switching off the ultrasonic source), and the dynamics of the change are shown in Fig. 12.

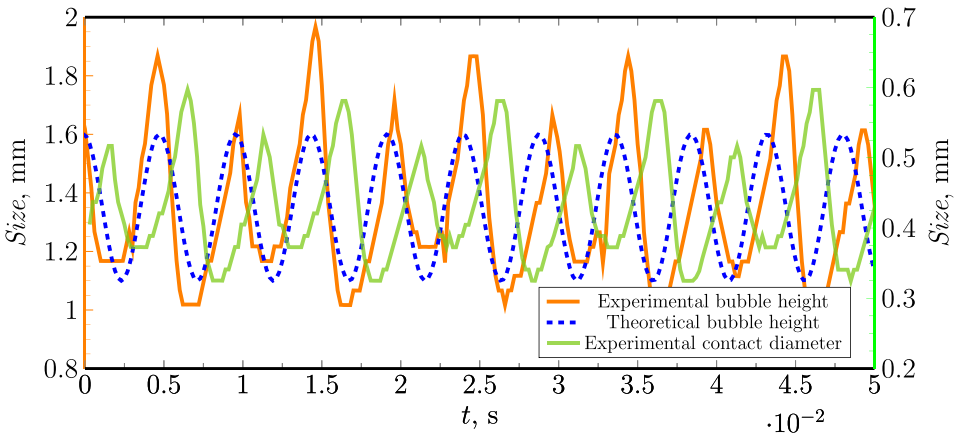


Fig. 10 Temporal dynamics of changes in the contact diameter and height of a bubble on an acrylic surface under ultrasonic exposure for the initial stage; comparison of experimental data on oscillations in bubble height with the formula (2) for the shape mode 2 eigen oscillation frequency of an inviscid, compressible bubble on the acrylic surface in a liquid

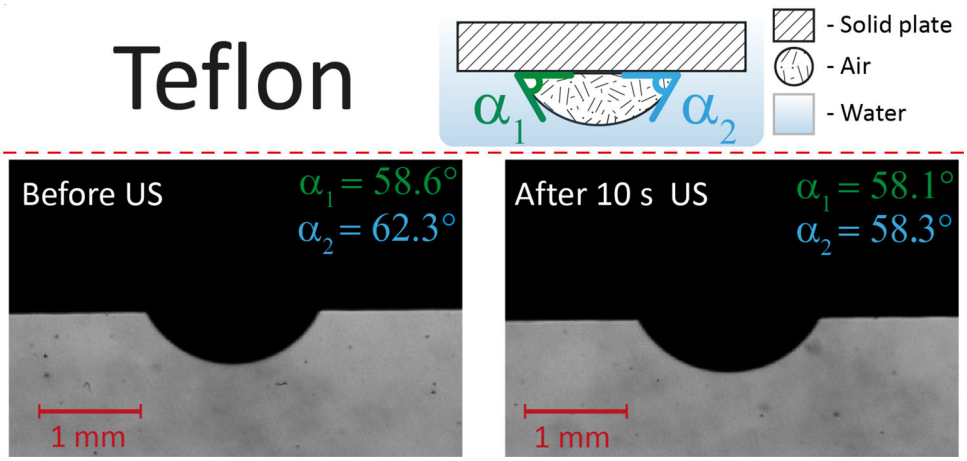


Fig. 11 Changing the wetting angle as a result of 10-s ultrasonic exposure on the surface of Teflon

The pattern observed in the experiment is quite complex: both eigen oscillations (of shape and volume) and forced (also of shape and volume) occur. Forced oscillations (including breathing mode), unlike the eigen ones, occur with the frequency of excitation.

We think that the "noise" in Fig. 12 is related to the breathing mode of eigen oscillations. Their frequency can be estimated using the formula for a compressible bubble, given, for example, in the article [46]. With the experimental parameters, the eigen oscillation frequency of the breathing mode is approximately 1000 Hz, which corresponds to the experimental data shown in Fig. 12.

The results of experiments conducted with the Teflon surface also made it possible to determine the oscillation frequency of the bubble surface (Fig. 13): for a bubble with a diameter of $d = 1.61$ mm, it turned out to be 204 Hz, which is close to the theoretical value according to that obtained from the formula (2) for the eigen oscillation frequency of the bubble shape.

It was also revealed that during the experiment with a duration of 5 min, the diameter of the bubble increased (this is shown in Fig. 15), which is related to its movement on a solid surface. The increase in bubble size under the influence of ultrasound is associated with into two different mechanisms [49]: rectified diffusion and coalescence. At the same time, the growth of the bubble size due to coalescence occurs faster than due to diffusion. Thus, on the surface of the submerged plate, a certain number of microbubbles [24] are formed, and when they come into contact with a larger bubble under the action of ultrasound, they coalesce, thereby increasing the size of the study bubble.

When the diameter of the bubble increases, the frequency of its eigen oscillations of the shape decreases. In experiments, the bubble diameter increased from $d = 1.61$ mm to $d = 2.6$ mm (Figs. 14, 14) in 5 min of US exposure. Along with that, the frequency of its oscillations decreased from 204 Hz to 100 Hz. This well corresponds to the change in eigen oscillation frequency with the increase of its diameter predicted by Eq. (2).

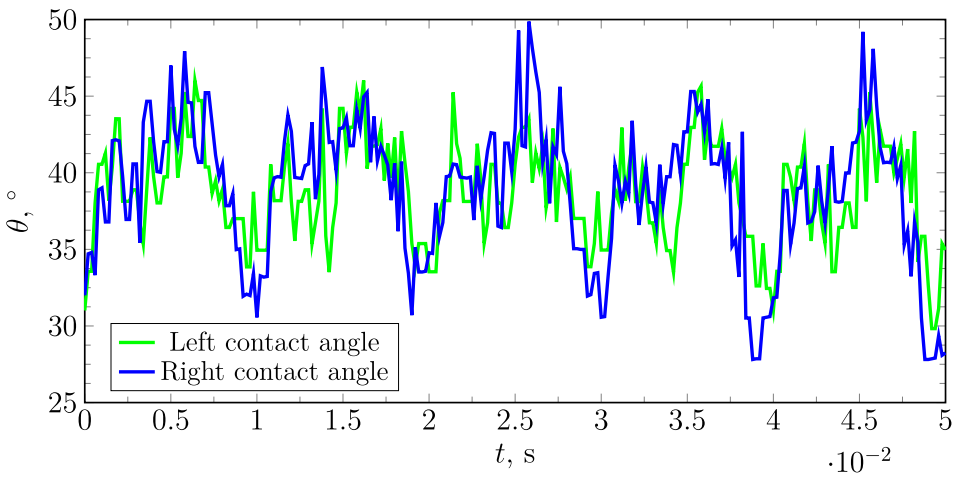


Fig. 12 Temporal dynamics of changes in the left and right contact angles on the surface of Teflon under ultrasonic exposure

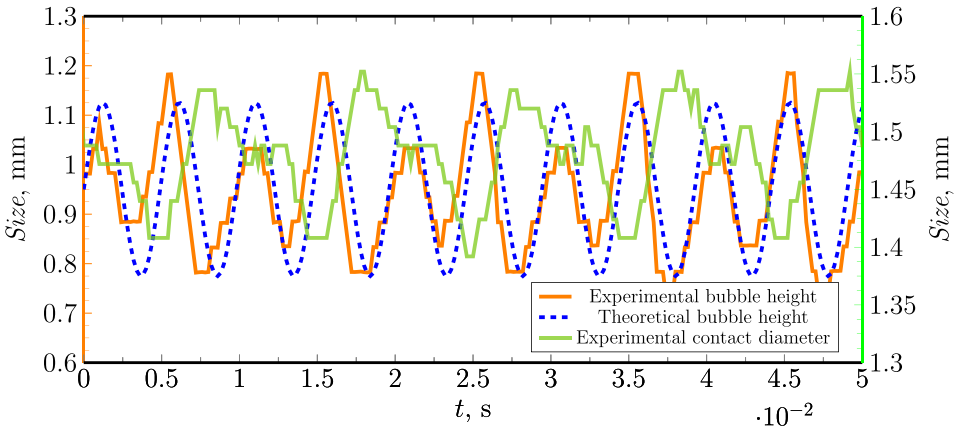


Fig. 13 Temporal dynamics of changes in the contact diameter and height of a bubble on a Teflon surface under ultrasonic exposure for the initial stage; comparison of experimental data on oscillations in bubble height with the formula (2) for shape mode 2 eigen oscillation frequency of an inviscid, compressible bubble on the Teflon surface in a liquid

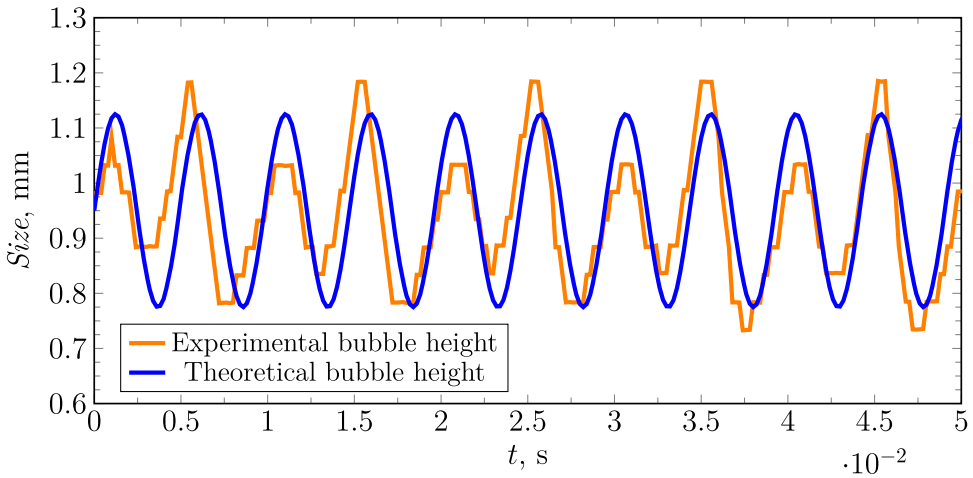


Fig. 14 Comparison of experimental data on fluctuations in the height of a bubble on the surface of Teflon with the theoretical value of shape mode 2 eigen oscillation frequency of the shape of a compressible, inviscid bubble, with a diameter of $d = 1.61$ mm

4 Conclusion

The effect of ultrasound on the behavior of an air bubble in a liquid near solid plates with different degrees of wettability (quartz glass, acrylic and Teflon) has been experimentally investigated using the captive bubble method. The bubble with a diameter 1–2 mm was generated using a capillary at a short distance from the plate, after which, under the influence of lift force, it approached a horizontally positioned solid plate.

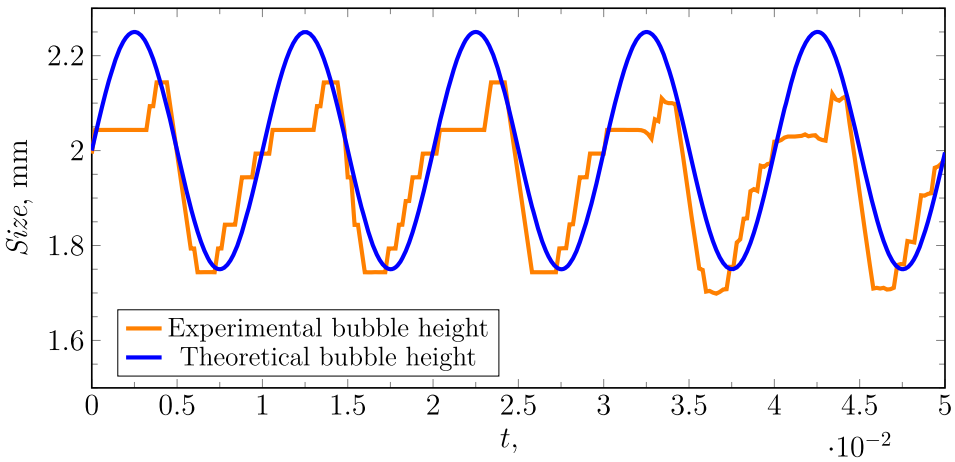


Fig. 15 Comparison of experimental data on fluctuations in bubble height on Teflon surface with theoretical value of shape mode 2 eigen oscillation frequency of the shape of a compressible, inviscid bubble. This graph shows the end of the experiment, which results in the decrease of frequency of height fluctuations by a factor of 2 due to increase in diameter to $d = 2.6\,\text{mm}$

Experiments have shown that in the case of a relatively hydrophilic quartz glass plate (the static contact angle is $130^\circ \div 145^\circ$), the bubble does not fix on a solid surface, and a thin liquid layer remains between them. Since the sound pressure along the plate is non-uniform due to the geometry of the ultrasonic field from the source and the reflection of ultrasonic waves from the walls of the vessel, under the action of ultrasound, the bubble first moves along the plate to the low-pressure area. Upon reaching this area, it performs translational oscillations in the vertical direction, approaching and moving away from the plate, accompanied by oscillations of the bubble surface.

In the case of an acrylic plate with a surface that is worse wetted with water than the surface of quartz glass (the static contact angle is $92^\circ \div 102^\circ$), the bubble is able to fix itself on a solid surface. Under the influence of ultrasound, at first, as in the case of quartz glass, it shifts along the plate to the area of low acoustic pressure, but then, unlike quartz glass, it does not make translational oscillations in the vertical direction near the plate, but is fixed on its surface, after which only oscillations of the bubble surface are observed.

Teflon is the most hydrophobic of the surfaces used in the experiments (the static contact angle is $65^\circ \div 75^\circ$). Qualitatively, the behavior of the bubble under the action of ultrasound on the surface of Teflon is similar to the behavior on the surface of acrylic.

In experiments with bubbles fixed on the surfaces of acrylic and Teflon, changes in contact diameter, bubble height, and dynamic contact angle were recorded over time using a high-speed camera. Processing of the measurement results showed that for short periods (about $10^{-2}\,\text{s}$), oscillations of all these characteristics are observed near some average values with a frequency close to the frequency equal to the frequency of shape mode 2 eigen oscillations for a spherical bubble, and oscillations in the contact diameter and height of the bubble occur in antiphase.

At long times, there is a change in the volume of the bubble due to rectification diffusion and coalescence with small bubbles formed on the surface of the plate and in the volume of the liquid under the influence of ultrasound. The frequency of oscillations of the contact diameter, the height of the bubble and the dynamic contact angle of the bubble with the radius increased as a result of these effects also agrees well with the formula for the frequency of natural oscillations of the spherical bubble shape.

The effect of ultrasound on the static contact angle has also been investigated. For this purpose, measurements of the static contact angle were carried out before exposure to ultrasound and after 10 s of exposure to ultrasound, its shutdown and subsequent relaxation for 2 s. It turned out that, both in the case of acrylic glass and in the case of Teflon, exposure to ultrasound leads to a decrease in the static contact angle.The reason for the decrease in the contact angle may be in that the bubble oscillations enable the contact line to pin to stronger defects in the solid structure and in the bubble mean shape deformation in ultrasound field (bubble flattening in the direction of ultrasound wave propagation).

The results obtained are important for applications in the field of flotation of mineral raw materials, since in the process of flotation, the formation of an air bubble–solid mineral particle complex plays a decisive role and therefore the search for an effective and environmentally safe way to control the interaction of a bubble with a solid surface, including using external fields, is a promising area of research.

Data availability statement Data sets generated during the current study are available from the corresponding author on reasonable request.

References

1. T. Wang, G. Liang, L. Li, S. Zhou, S. Shen, Droplet wetting propagation on a hybrid-wettability surface. Langmuir **37**(39), 11646–11656 (2021). https://doi.org/10.1021/acs.langmuir.1c02255
2. K.J. Kubiak, M.C.T. Wilson, T.G. Mathia, P. Carval, Wettability versus roughness of engineering surfaces. Wear **271**(3), 523–528 (2011). https://doi.org/10.1016/j.wear.2010.03.029. (**The 12th International Conference on Metrology and Properties of Engineering Surfaces**)
3. J.K. Day, A study of bubble wetting on surfaces. PhD thesis, Massachusetts Institute of Technology (2010)
4. H. Fujii, T. Matsumoto, S. Izutani, S. Kiguchi, K. Nogi, Surface tension of molten silicon measured by microgravity oscillating drop method and improved sessile drop method. Acta Mater. **54**(5), 1221–1225 (2006). https://doi.org/10.1016/j.actamat.2005.10.058
5. D. Brutin, Z. Zhu, O. Rahli, J. Xie, Q. Liu, L. Tadrist, Sessile drop in microgravity: creation, contact angle and interface. Microgravity Sci. Technol. **21**(1), 67–76 (2009). https://doi.org/10.1007/s12217-009-9132-x
6. J.-W. Song, L.-W. Fan, Temperature dependence of the contact angle of water: a review of research progress, theoretical understanding, and implications for boiling heat transfer. Adv. Colloid Interface Sci. **288**, 102339 (2021). https://doi.org/10.1016/j.cis.2020.102339
7. Y.-T. Liu, H.-M. Li, M.-Z. Gao, S.-Q. Ye, Y. Zhao, J. Xie, G.-K. Liu, J.-J. Liu, L.-M. Li, J. Deng et al., Experimental and molecular dynamics study into the surfactant effect upon coal wettability. RSC Adv. **11**(40), 24543–24555 (2021)
8. K. Gao, H. Liu, L. Sun, Z. Zhang, Effect of gas input conditions and ultrasound on the dynamic behavior of flotation bubbles. ACS Omega **7**(26), 22326–22340 (2022). https://doi.org/10.1021/acsomega.2c01162
9. D. Lyubimov, L. Klimenko, T. Lyubimova, L. Filippov, The interaction of a rising bubble and a particle in oscillating fluid. J. Fluid Mech. **807**, 205–220 (2016). https://doi.org/10.1017/jfm.2016.608
10. L.O. Filippov, I.V. Filippova, O. Barres, T.P. Lyubimova, O.O. Fattalov, Intensification of the flotation separation of potash ore using ultrasound treatment. Miner. Eng. **171**, 107092 (2021). https://doi.org/10.1016/j.mineng.2021.107092
11. J.B. Bostwick, P.H. Steen, Response of driven sessile drops with contact-line dissipation. Soft Matter **12**(43), 8919–8926 (2016). https://doi.org/10.1039/C6SM01928E
12. D. Ding, J. Bostwick, Oscillations of a partially wetting bubble. J. Fluid Mech. **945**, 24 (2022). https://doi.org/10.1017/jfm.2022.584
13. D.V. Lyubimov, T.P. Lyubimova, S.V. Shklyaev, Behavior of a drop on an oscillating solid plate. Phys. Fluids (2006). https://doi.org/10.1063/1.2137358
14. A. Ivantsov, T. Lyubimova, G. Khilko, D. Lyubimov, The shape of a compressible drop on a vibrating solid plate. Mathematics **11**(21), 4527 (2023). https://doi.org/10.3390/math11214527
15. J.A. Sarasua, L.R. Rubio, E. Aranzabe, J.L.V. Vilela, Energetic study of ultrasonic wettability enhancement. Ultrason. Sonochem. **79**, 105768 (2021). https://doi.org/10.1016/j.ultsonch.2021.105768
16. R. Galleguillos-Silva, Y. Vargas-Hernández, L. Gaete-Garretón, Wettability of a surface subjected to high frequency mechanical vibrations. Ultrason. Sonochem. **35**, 134–141 (2017). https://doi.org/10.1016/j.ultsonch.2016.09.011
17. V. Bjerknes, *Die Kraftfelder* (University of Michigan Library, Michigan, 1909)
18. K. Yoshida, T. Fujikawa, Y. Watanabe, Experimental investigation on reversal of secondary Bjerknes force between two bubbles in ultrasonic standing wave. J. Acoust. Soc. America **130**(1), 135–144 (2011). https://doi.org/10.1121/1.3592205
19. J. Jiao, Y. He, S.E. Kentish, M. Ashokkumar, R. Manasseh, J. Lee, Experimental and theoretical analysis of secondary Bjerknes forces between two bubbles in a standing wave. Ultrasonics **58**, 35–42 (2015). https://doi.org/10.1016/j.ultras.2014.11.016
20. Y. Zhang, S. Li, The secondary Bjerknes force between two gas bubbles under dual-frequency acoustic excitation. Ultrason. Sonochem. **29**, 129–145 (2016). https://doi.org/10.1016/j.ultsonch.2015.08.022
21. T. Leong, M. Ashokkumar, S. Kentish, The growth of bubbles in an acoustic field by rectified diffusion, in *Handbook of Ultrasonics and Sonochemistry*, vol. 1, (Springer, Singapore, 2016), pp.69–98. https://doi.org/10.1007/978-981-287-278-4_2
22. L. Jin, W. Wang, Y. Tu, K. Zhang, Z. Lv, Effect of ultrasonic standing waves on flotation bubbles. Ultrason. Sonochem. **73**, 105459 (2021). https://doi.org/10.1016/j.ultsonch.2020.105459
23. D.V. Lyubimov, T.P. Lyubimova, A.A. Cherepanov, Resonance oscillations of a drop (bubble) in a vibrating fluid. J. Fluid Mech. **909**, 18 (2021). https://doi.org/10.1017/jfm.2020.949
24. L. Wang, X. Wang, L. Wang, J. Hu, C.L. Wang, B. Zhao, X. Zhang, R. Tai, M. He, L. Chen et al., Formation of surface nanobubbles on nanostructured substrates. Nanoscale **9**(3), 1078–1086 (2017). https://doi.org/10.1039/C6NR06844H
25. O. Fattalov, T. Lyubimova, K. Rybkin, I. Lunegov, M. Kuchinskiy, Experimental study of cavitation erosion of quartz in the presence of surfactant molecules. J. Phys. Conf. Ser. **1809**, 012019 (2021). https://doi.org/10.1088/1742-6596/1809/1/012019
26. V.V. Kalmykov, E.A. Medvedeva, R. Konozobko, Methods for estimating the edge angle by the lying drop method. Electron. J. Sci. Technol. Educ. **5**(1), 51–56 (2020). https://doi.org/10.1039/C6SM01928E
27. C. Extrand, Uncertainty in contact angle measurements from the tangent method. J. Adhes. Sci. Technol. **30**(15), 1597–1601 (2016). https://doi.org/10.1021/la0268350
28. T.G. Leighton, A.J. Walton, An experimental study of the sound emitted from gas bubbles in a liquid. Eur. J. Phys. **8**(2), 98 (1987)

29. S.K. Bhangu, M. Ashokkumar, Theory of sonochemistry, in *Sonochemistry from Basic Principles to Innovative Applications*. (Springer, Cham, 2017), pp.1–28
30. E.D. Manev, A.V. Nguyen, Critical thickness of microscopic thin liquid films. Adv. Colloid Interface Sci. **114**, 133–146 (2005). https://doi.org/10.1016/j.cis.2004.07.013
31. E. Lifshitz, The theory of molecular attractive forces between solid bodies. J. Exp. Theor. Phys. USSR **29**, 83–94 (1955)
32. L. Xie, J. Wang, Q. Lu, W. Hu, D. Yang, C. Qiao, X. Peng, Q. Peng, T. Wang, W. Sun et al., Surface interaction mechanisms in mineral flotation: Fundamentals, measurements, and perspectives. Adv. Colloid Interface Sci. **295**, 102491 (2021). https://doi.org/10.1016/j.colsurfa.2023.131210
33. M. Krasowska, K. Malysa, Kinetics of bubble collision and attachment to hydrophobic solids: I. effect of surface roughness. Int. J. Miner. Process. **81**(4), 205–216 (2007). https://doi.org/10.1016/j.minpro.2006.05.003
34. K. Malysa, M. Krasowska, M. Krzan, Influence of surface active substances on bubble motion and collision with various interfaces. Adv. Colloid Interface Sci. **114**, 205–225 (2005). https://doi.org/10.1016/j.cis.2004.08.004
35. M. Kuchinskiy, T. Lyubimova, K. Rybkin, O. Fattalov, L. Klimenko, Experimental and numerical study of acoustic pressure distribution in a sonochemical reactor. J. Phys. Conf. Ser. **1809**, 012025 (2021). https://doi.org/10.1088/1742-6596/1809/1/012025
36. A. Keshmiri, S. Heitkam, A. Bashkatov, M. Eftekhari, K. Eckert, B. Keshavarzi, Surfactant sorption on a single air bubble in an ultrasonic standing acoustic wave field. Colloids Surf. A: Physicochem. Eng. Asp. **665**, 131210 (2023). https://doi.org/10.1016/j.colsurfa.2023.131210
37. Z. Wei, L.K. Weavers, Combining comsol modeling with acoustic pressure maps to design sono-reactors. Ultrason. Sonochem. **31**, 490–498 (2016). https://doi.org/10.1016/j.ultsonch.2016.01.036
38. C.W. Extrand, Contact angles and hysteresis on surfaces with chemically heterogeneous islands. Langmuir **19**(9), 3793–3796 (2003). https://doi.org/10.1021/la0268350
39. E. Decker, B. Frank, Y. Suo, S. Garoff, Physics of contact angle measurement. Colloids Surf. A: Physicochem. Eng. Asp. **156**(1–3), 177–189 (1999)
40. M.A. Trapuzzano, Controlled wetting using ultrasonic vibration. PhD thesis, University of South Florida (2019)
41. M. Trapuzzano, A. Tejada-Martínez, R. Guldiken, N. Crane, Volume and frequency-independent spreading of droplets driven by ultrasonic surface vibration. Fluids **5**(1), 18 (2020). https://doi.org/10.3390/fluids5010018
42. E.V. Skorb, D.G. Shchukin, H. Möhwald, D.V. Andreeva, Ultrasound-driven design of metal surface nanofoams. Nanoscale **2**(5), 722–727 (2010). https://doi.org/10.1039/C0NR00074D
43. Y. Zhukova, S.A. Ulasevich, J.W. Dunlop, P. Fratzl, H. Möhwald, E.V. Skorb, Ultrasound-driven titanium modification with formation of titania based nanofoam surfaces. Ultrason. Sonochem. **36**, 146–154 (2017). https://doi.org/10.1016/j.ultsonch.2016.11.014
44. M.D. Sosa, M.L.M. Ricci, L.L. Missoni, D.H. Murgida, A. Cánneva, N.B. D'Accorso, R.M. Negri, Liquid-polymer triboelectricity: chemical mechanisms in the contact electrification process. Soft Matter **16**(30), 7040–7051 (2020). https://doi.org/10.1039/D0SM00738B
45. X. Li, L. Zhang, Y. Feng, Y. Zhang, H. Xu, F. Zhou, D. Wang, Visualization of charge dynamics when water droplets bounce on a hydrophobic surface. ACS Nano (2023). https://doi.org/10.1021/acsnano.3c08742
46. S. Shklyaev, A. Straube, Linear oscillations of a compressible hemispherical bubble on a solid substrate. Phys. Fluids **20**(5), 052102 (2008). https://doi.org/10.1063/1.2918728
47. C.A. Miller, L.E. Scriven, The oscillations of a fluid droplet immersed in another fluid. J. Fluid Mech. **32**(3), 417–435 (1968). https://doi.org/10.1017/S0022112068000832
48. A. Aganin, M. Ilgamov, L. Kosolapova, V.G. Malakhov, Nonlinear non-spherical fluctuations of a gas bubble with periodic changes in the pressure of the surrounding liquid. Thermophys. Aeromech. **15**(3), 521–533 (2008)
49. T. Leighton, *The Acoustic Bubble* (Academic press, California, 2012)

Springer Nature or its licensor (e.g. a society or other partner) holds exclusive rights to this article under a publishing agreement with the author(s) or other rightsholder(s); author self-archiving of the accepted manuscript version of this article is solely governed by the terms of such publishing agreement and applicable law.